1983

THERMODYNAMIC AND STRUCTURAL PROPERTIES OF MeV ION BEAM AMORPHIZED SILICON

S. Roorda[1], W.C. Sinke[1], J.M. Poate[2], D.C. Jacobson[2], P. Fuoss[3], S. Dierker[2], B.S. Dennis[2] and F. Spaepen[4].
1) FOM-Institute for Atomic and Molecular Physics, Kruislaan 407, 1089 SJ Amsterdam, The Netherlands.
2) AT&T Bell Laboratories, Murray Hill, NJ 07974, USA.
3) AT&T Bell Laboratories, Holmdel, NJ 07733, USA.
4) Harvard University, Cambridge, MA 02138, USA

ABSTRACT

Thermodynamic and structural properties of amorphous Si (a-Si), prepared by MeV $^{28}Si^{+}$-ion implantation are investigated by differential scanning calorimetry, Raman spectroscopy and X-ray diffraction. The influence of thermal annealing below 500 °C on a-Si is investigated with these different probes. The observed changes result from structural relaxation. Raman spectroscopy and X-ray diffraction show that structural relaxation is accompanied by changes in the average atomic structure.

INTRODUCTION

The thermodynamic properties [1] of amorphous Si (a-Si) represent an intriguing illustration of the importance of short and intermediate range order on the physical properties of amorphous solids [2]. For example, although crystalline Si (c-Si) and a-Si consist of the same, covalently bonded atoms with very similar local structure, the first-order melting transition in a-Si occurs at a temperature that is more than 200 K below that of c-Si [3]. Similarly, the enthalpy of a-Si has been observed to be variable, and to depend on the thermal history of the material [4,5]. 'Structural relaxation' has been suggested to be an intrinsic property of a disordered material. However, it has recently been discovered that a similar phenomenon (a heat release upon low temperature annealing) also occurs in c-Si which is very heavily damaged [6]. Thus, an investigation into the nature of structural relaxation can teach us the extent to which properties of solids are determined by the presence or absence of crystalline order.

To date, such studies have mostly dealt with a-Si which was prepared by methods such as sputtering or vacuum evaporation. When a-Si is prepared in this way, the resulting material can contain macroscopic voids and/or trapped gas [7]. This means that some of the observed property changes of a-Si may not be governed by the atomic structure, but by macroscopic morphology. Preparation of a-Si by implantation of c-Si with Si^{+} ions is a way to form ultra-clean a-Si which is free of macroscopic voids. Only recently have high-current, high energy heavy ion accelerators become available which make it possible to prepare a-Si in the amounts necessary for calorimetry.

In this study we have characterized a-Si, prepared by self-implantation of c-Si, which was brought to several stages of structural relaxation. A variety of experimental probes was used: differential scanning calorimetry (DSC) as well as isothermal calorimetry (DIC), Raman spectroscopy (Raman), X-ray diffraction (XRD), and density measurements [8].

SAMPLE PREPARATION AND EXPERIMENTAL PROCEDURES

Crystalline (100) Si targets were implanted with $^{28}Si^{+}$ ions of 0.5, 1 and 2 MeV to a dose of 5×10^{15} ions/cm^2 for each energy, using the NEC 1.8 MeV tandem accelerator at AT&T. The ion beam was defocussed to a spot size of $\approx$1cm^2 and rastered electrostatically over the surface of the targets. During implantation, the targets were held at liquid nitrogen temperature. In order to prevent beam heating effects, the total power on target never exceeded 10 W. This treatment resulted in the formation of $\approx$2.2 μm thick a-Si layers (as determined by RBS/channeling of 1 MeV H^{+} using stopping powers which were scaled from the stopping power of D^{+} in Si [9]). For DSC measurements, double sided polished c-Si discs of 7.6 mm diameter and 100 μm thickness were used. Both sides were implanted. Before implantation, the samples were annealed

cm^2 were implanted with the above mentioned recipe, and in addition to this with $^{28}Si^+$ ions of 3.5 and 5 MeV to doses of 6 and 7×10^{15} ions/cm^2, respectively. As a result of these extra implantations, the thickness of the a-Si layer increased to ≈3.6 µm. After implantation, the samples were divided in 6 sets. Five sets were annealed at temperatures of 150, 230, 300, 400 and 500 °C for 45 minutes in vacuum. The sixth set was not annealed (as-implanted).

DSC measurements were performed on a Perkin-Elmer DSC-2, equipped with a new and stable measurement head and a PC for data-acquisition. This, and the fact that each measurement could be done using at least 3 double-sided implanted discs, made it possible to measure with exceptional accuracy. During the measurements the Si samples rested on graphite liners and the reference DSC-pan was loaded with the same number of unimplanted c-Si discs to balance the thermal load of the furnaces. Each scan was taken after an initial waiting period of several minutes to allow the DSC to reach equilibrium following loading of the samples. When the DSC had reached the end temperature, it was held at that temperature for a short period to record the isotherm, and then cooled back rapidly to the start temperature. Subsequently, the DSC was allowed to equilibrate again and a second scan of the same samples was made using the same procedure. Subtraction of the second scan from the first one gives the heat release during the first scan. Isothermal measurements of the heat release kinetics were made at 200, 350 and 500 °C using 6 double-sided implanted discs which did not receive any post-implantation heat treatment. The DSC was calibrated using the melting point of In and a solid-solid phase transition in K_2CrO_4 for the temperature scale and the specific heat of pure sapphire for the power scale.

Raman measurements were done using the 488 nm line from an Ar laser, keeping the power on the sample below 150 mW. The laser was focused to a rectangular spot of ≈50x200 µm. A triple stage monochromator dispersed the Raman spectrum on a CCD camera which allowed one spectrum to be recorded with sufficient statistics in 2 minutes. X-ray diffraction was performed at the Brookhaven NSLS. During the XRD measurements the samples were held in vacuum to prevent air scattering. The diffracted beam was analyzed by a channel-cut crystal monochromator.

RESULTS AND DISCUSSION

Isothermal Calorimetry - Fig. 1 shows DIC difference traces at 200, 350 and 500 °C. The

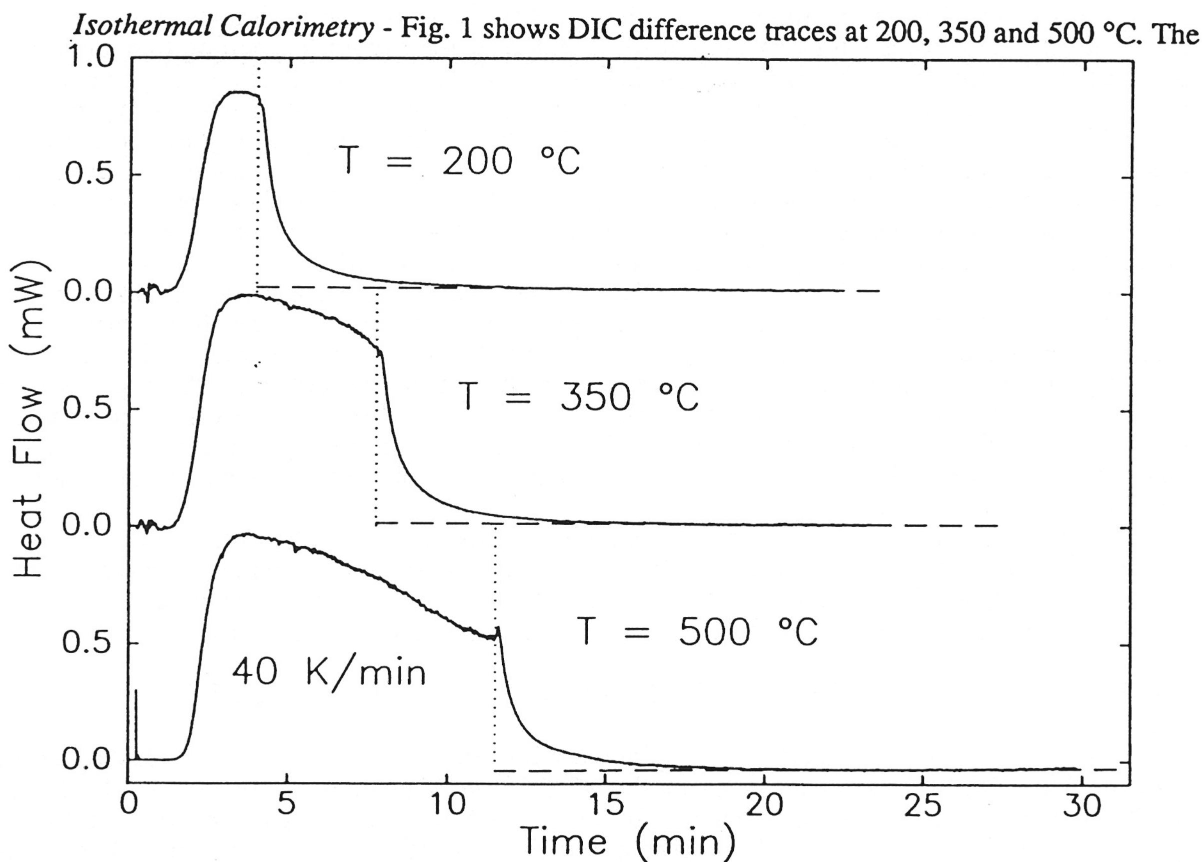

Figure 1. DSC and DIC difference traces of as-implanted a-Si. Dotted lines serve to separate the DSC and DIC signals. Dashed lines are discussed in the text.

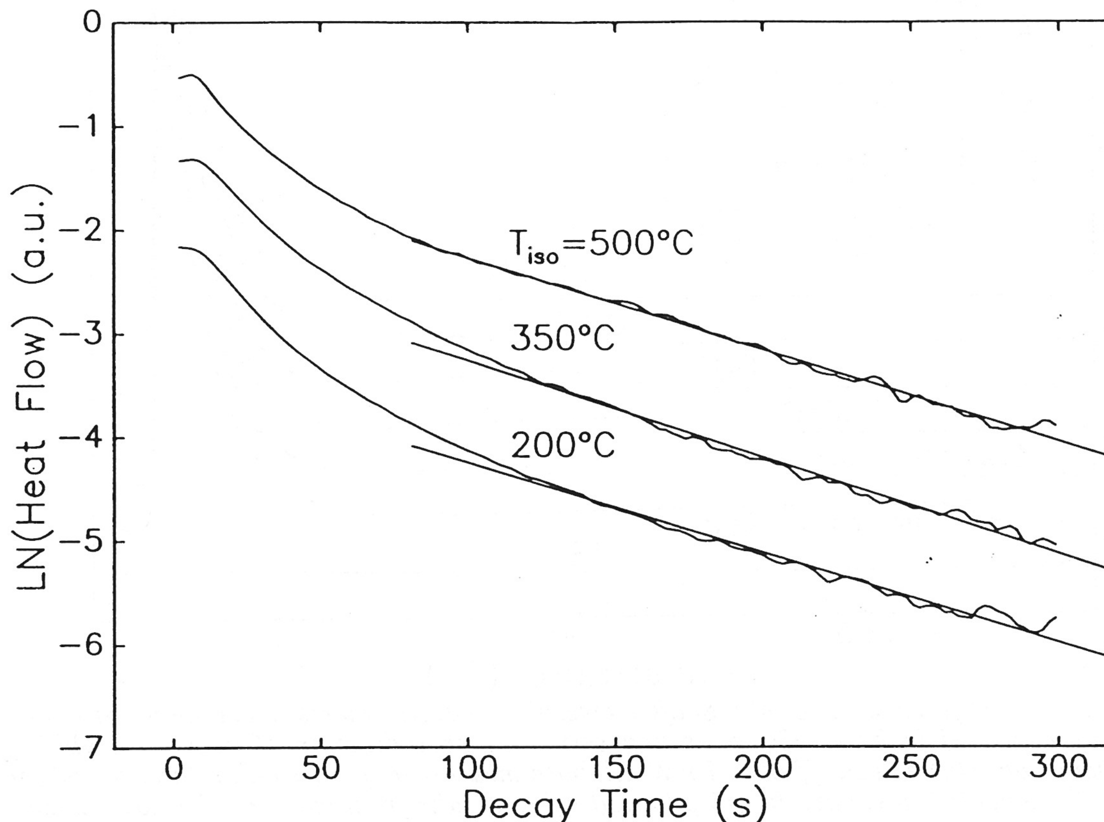

Figure 2. DIC curves from Fig. 1, displayed on a logarithmic scale. Only the first 5 minutes are shown, and curves are offset for clarity.

DSC difference signals which were recorded during heating (at 40 K/min) to the end temperature, are also shown. After 10 minutes, all three isotherms have stabilized. Linear least squares fits have been made to the part of the isotherms, corresponding to times longer than 10 minutes. These fits were extrapolated back to the beginpoint of the isotherms and define the isothermal baseline (shown as dashed lines in Fig.1). Subtraction of these baselines from the corresponding measured traces yields the transient heat release, which can now be studied in detail.

Fig. 2 shows the natural logarithm of the isothermal heat release decay signal as a function of time (curves have been offset for clarity). It is observed that for longer times the data can be described by a straight line, but initially the decay is much faster. This indicates that several processes, each with a different decay time, contribute to the heat release. After the fast processes have died out, the decay is dominated by the slowest process that still runs (at a measurable rate) at the temperature under consideration. The values for the characteristic time of these processes can be determined from the slope of the fits in Fig. 2 and are found to be 113, 107 and 115 s at 200, 350 and 500 °C, respectively.

Structural relaxation can be described by a spectrum of processes according to an expression of the form [10] $P(t) = P_\infty + \Sigma_i P_i \bullet \exp(-t/\tau_i)$, where P(t) is a measured property, P_∞ and P_i are constant and the characteristic times t_i obey an Arrhenius-type behaviour of the form $\tau_i = \tau_0 \bullet \exp(E_i/kT)$. In the latter expression, E_i is the activation energy of a process which exhibits a characteristic time τ_i for relaxation. Assuming that τ_0 is simply given by h/kT, with h and k the constants of Planck and Boltzmann, respectively, the above characteristic times can be used to estimate the activation energy of the dominant processes at each of the studied temperatures. It is found that τ_i is almost independent of temperature, therefore, at higher temperatures processes with larger activation energy are probed. The above determined values for τ_i correspond to values for E_i of 1.4, 1.9 and 2.3 eV at 200, 350 and 500 °C, respectively.

TABLE I Total enthalpy difference ΔH_{ac} between a-Si and c-Si, and Raman TO-like peak width $\Delta\Theta$ for several a-Si preanneal temperatures.

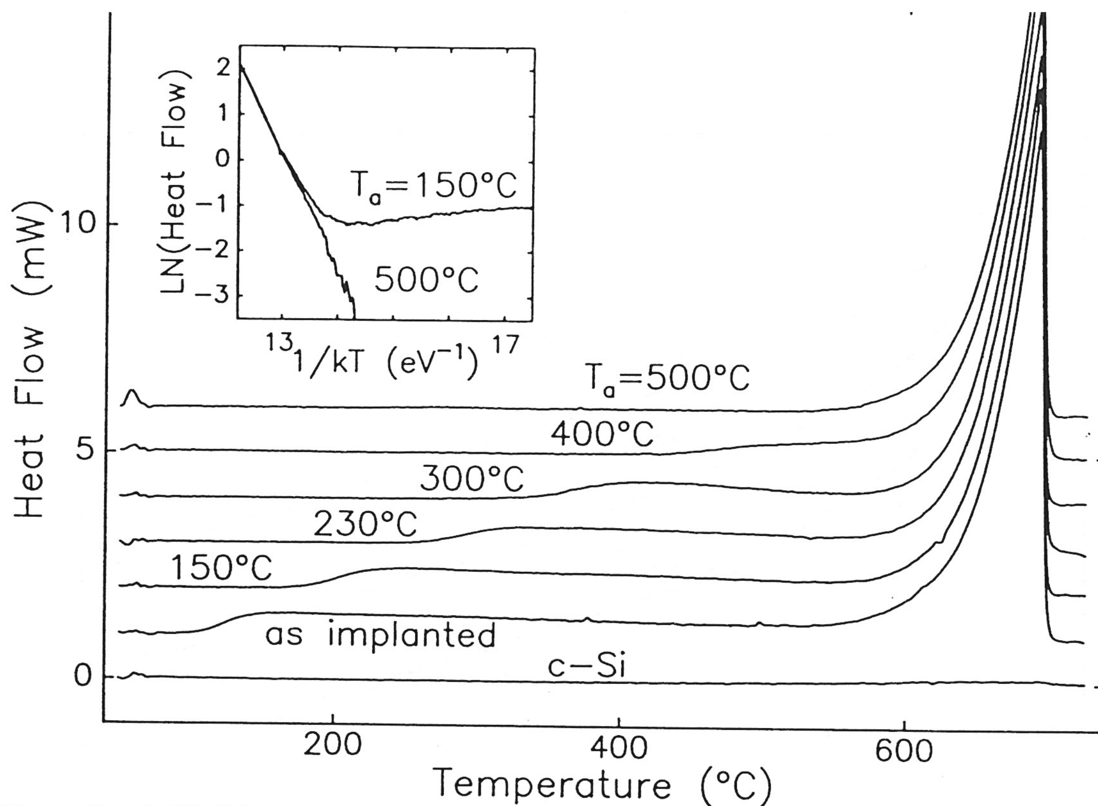

Figure 3. DSC difference traces of a-Si after several anneal treatments. The bottom curve was measured with c-Si in both DSC-pans and serves as an indication of baseline stability. Subsequent traces have been offset by 1 mW. All baselines, except for the c-Si reference and for the 500 °C annealed a-Si have been optimized using results from isothermal measurements displayed in Figure 1. The inset shows two traces from the same set in an Arrhenius fashion.

Differential Scanning Calorimetry - The traces in Fig. 1 and 2 were extrapolated back to t=0. Thus the instantaneous heat flow at the end of the scanning trace could be determined independent of the scanned full baseline. The values for the intantaneous heat flow were 8.8, 7.5 and 5.6 ± 0.1 W/mol , at 200, 350 and 500 °C, respectively. These values, which are essentially independent of the scanned baseline may be used as 'anchorpoints' to (re-)construct the most accurate baseline for DSC scans over a wide temperature range where accurate measurements are limited by baseline stability.

Six such scans are shown in Fig. 3. DSC difference traces over the full instrumental temperature range are shown for a-Si annealed in vacuum at 6 different temperatures. For each curve a baseline has been constructed by lineair interpolations between the anchorpoints, and from the anchorpoints to the nearest zero-signal point (i.e. below the preanneal temperature or after complete crystallization) of the measured curve. The inset in Fig. 3 is an Arrhenius plot of two selected curves. It is observed that at high temperatures, heat flow is dominated by crystallization. From the slope of the lineair sections, the activation energy of SPE is determined and found to vary between 2.43 and 2.66 eV, in reasonable agreement with literature (2.7 eV [5,11]). Integration of the curves in Fig. 3 yields the total enthalpy difference ΔH_{ac} between c-Si and a-Si. This total enthalpy difference depends on thermal history of a-Si as is shown by the variation in ΔH_{ac} with preanneal temperature. All values of ΔH_{ac} are shown in Table I.

X-ray Diffraction - The variation in ΔH_{ac} upon annealing has been related to ordering on an atomic level, involving a decrease in average bond angle distortion $\Delta\Theta$ and/or removal of a large concentration of point defect complexes. Such ordering involving many atoms, is expected to result in changes in the X-ray diffraction pattern of a-Si. This has indeed been observed, as shown in Fig. 4. Three X-ray diffraction patterns are shown, corresponding to as-implanted and 230 and 500 °C annealed a-Si. It can be seen that the patterns show a clear difference in the height and width of the first peak. The position of the diffraction peaks is not affected by the anneal. The change in the intensity of the first peak corresponds to ordering on a scale beyond the nearest neighbour distance. The respective radial distribution functions show that the average

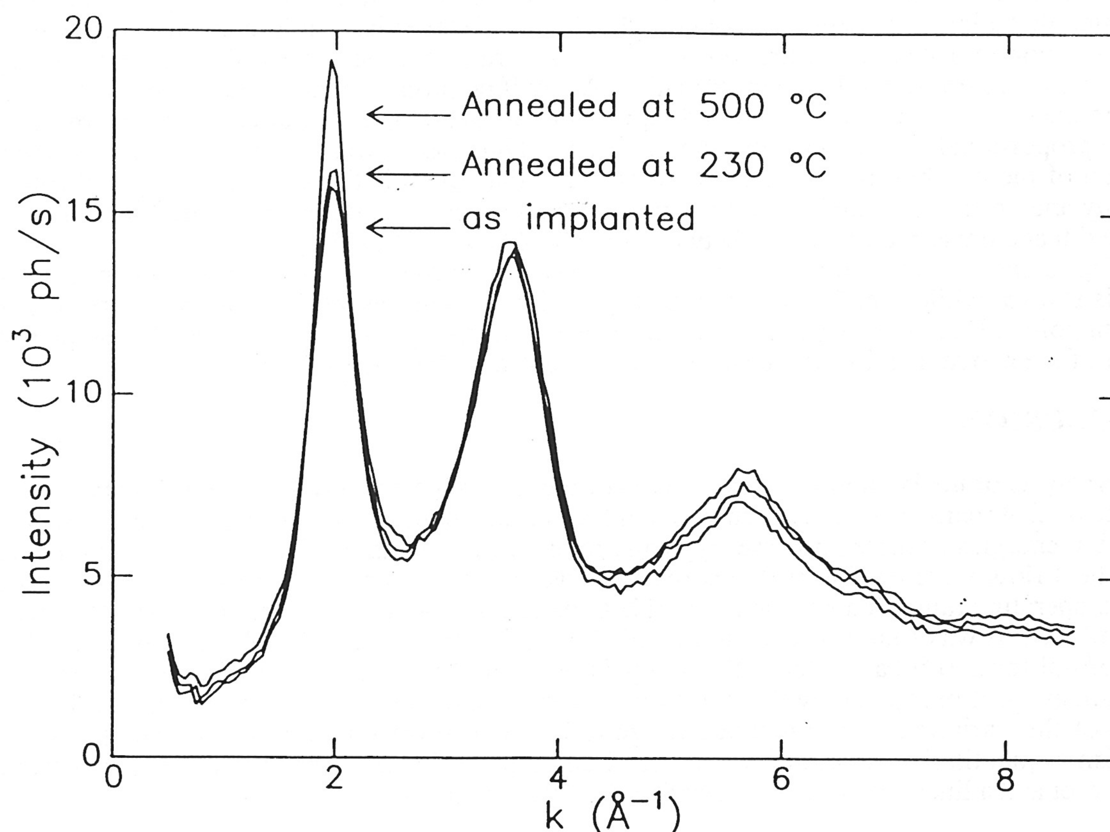

Figure 4. X-ray diffraction patterns of a-Si. Shown are the patterns for as-implanted, 230 °C annealed and 500 °C annealed a-Si.

nearest-neighbour distance does not change. Although these spectra have yet to be thoroughly analyzed, it can be concluded that annealing of a-Si indeed leads to reordering on an atomic level at an intermediate rather than short range.

Raman Spectroscopy - In order to quantitatively relate the observed variation of ΔH_{ac} to changes in the structure of a-Si, similarly treated a-Si samples were analyzed by Raman spectroscopy. The width of the TO-like peak in the Raman spectrum of a-Si has been argued to be roughly linearly dependent on the average bond angle distortion $\Delta\Theta$ [12]. The half-width $\Gamma/2$ at the high energy side was used, because at low wavenumbers, the TO-like peak overlaps with LO and LA like features. For all six flavours of a-Si, $\Gamma/2$ was determined. The results are listed in Table I.

Two possible relations between ΔH_{ac} and $\Gamma/2$ may be envisioned. 1) In a fully connected a-

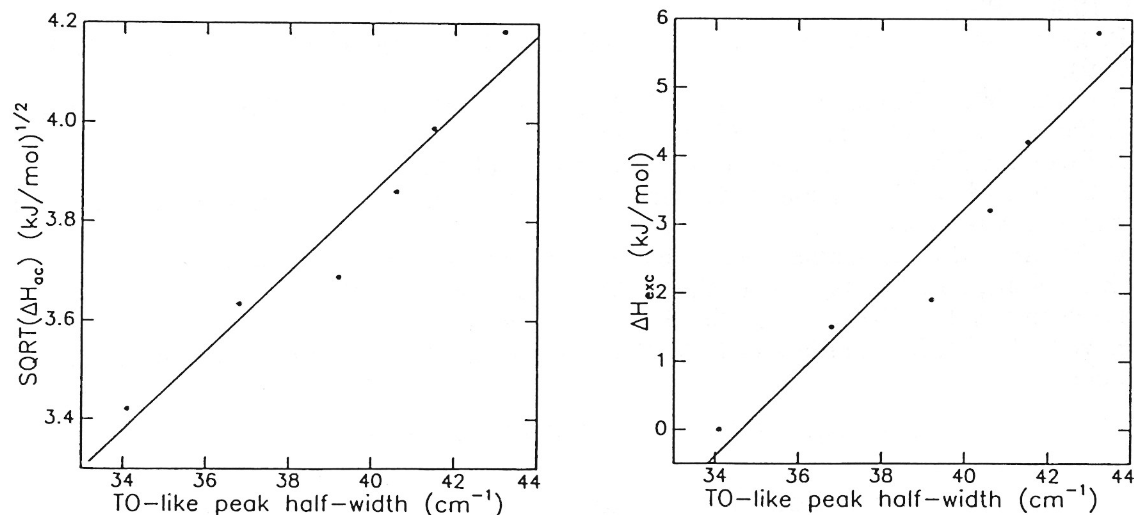

Figure 5. Relation between Raman parameter and enthalpy difference ΔH ... a) Square root of

been argued to be mainly strain energy from bond angle distortions. For a Keating-type potential, this energy is roughly proportional to the square of $\Delta\Theta$. Since $\Gamma/2$ depends linearly on $\Delta\Theta$, the relation between $\Delta\Theta$ and ΔH_{ac} can now, in principle, be tested. 2) Recently, it has been suggested that a large concentration of complex point defects exist in a-Si and that these defects play an important role in structural relaxation. In general, point defects in Si are surrounded by small strained regions. To first approximation, $\Delta\Theta$ will be proportional to the relative volume of strained material and, as long as strained regions do not overlap, the volume of strained material will be proportional to the concentration of defects. Thus $\Delta\Theta$ is, to first approximation, a linear function of the number of point defects. Assuming that ΔH_{ac} is the sum of the crystallization enthalpy and an excess enthalpy which is proportional to the point defect concentration, it is thus expected that a linear relation exists between $\Delta\Theta$ and $\Delta H_{exc}=\Delta H_{ac}-\Delta H_{cryst}$.

Fig. 5 shows ΔH_{ac} versus $\Gamma/2$ for all six flavours of a-Si. In Fig. 5 a) the square root of ΔH_{ac} is shown, while Fig. 5 b) displays ΔH_{exc}. Solid lines represent linear least squares fits to the data points. It is observed that both fits describe the data points equally well. Consequenty, neither of the above mentioned scenarios can be rejected on the basis of our results.

CONCLUSIONS

Analysis of the isothermal decay curves of the heat released during structural relaxation of a-Si shows that many processes, each with a different time constant, contribute to relaxation. The activation energies of these processes typically range from 1 to 2.5 eV. Isothermal measurements of the heat flow were used to (re)construct reliable baselines for DSC scans extending over a large temperature range. This made it possible to determine the total enthalpy difference between a-Si and c-Si. It was found that the total enthalpy varied from 16.6 kJ/mol for as implanted to 11.6 kJ/mol for 500 °C annealed a-Si. Analysis of similarly annealed a-Si by X-ray diffraction and Raman spectroscopy show that the average structure changes upon annealing, and that the nature of the variation is intermediate range rather then short range ordering. An attempt to establish a quantitative relation between total enthalpy and Raman peak width showed that a square root and a lineair dependence describe the data equally well.

ACKNOWLEDGEMENTS

Work at FOM was financially supported by the Nederlands Organisatie voor Wetenschappelijk Onderzoek (NWO) and the Stichting Technische Wetenschappen (STW). Work performed at Harvard was supported by the National Science Foundation through the Harvard Materials Research Laboratory under contract number DMR-86-14003.

REFERENCES

1 E.P. Donovan, F. Spaepen, D. Turnbull, J.M. Poate and D.C. Jacobson, Appl. Phys. Lett. **42**, 698 (1983).
2 R. Zallen, The Physics of Amorphous Solids (Wiley, New York, 1983).
3 M.O. Thompson, G.J. Galvin, J.W. Mayer, P.S. Peercy, J.M. Poate, D.C. Jacobson, A.G. Cullis and N.G. Chew, Phys. Rev. Lett. **52**, 2360 (1984).
4 S. Roorda, S. Doorn, W.C. Sinke, P.M.L.O. Scholte and E. van Loenen, Phys. Rev. Lett. **62**, 1880 (1989).
5 E.P. Donovan, F. Spaepen, J.M. Poate and D.C. Jacobson, Appl. Phys. Lett. **55**, 1516 (1989).
6 S. Roorda, W.C. Sinke, J.M. Poate, D.C. Jacobson, P. Fuoss, S. Dierker, B.S. Dennis, D.J. Eaglesham and F. Spaepen, *These Proceedings*.
7 J.C. Bean and J.M. Poate, Appl. Phys. Lett. **36**, 59 (1980).
8 J.S. Custer, M.O. Thompson, D.C. Jacobson, J.M. Poate, S. Roorda, W.C. Sinke and F. Spaepen, *These Proceedings*.
9 D.C. Santry and R.D. Werner, Nucl. Instrum. and Meth. **188**, 211 (1981).
10 M.R.J. Gibbs, J.E. Evetts, J.A. Leake, J. Mater. Sc. **18**, 278 (1983).
11 G.L.Olson and J.A. Roth, Mater. Sc. Rep. **3**, 1 (1988).
12 see: W.C. Sinke, S. Roorda and F.W. Saris, J. Mater. Res. **3**, 120 (1988) and references therein.

MATERIALS RESEARCH SOCIETY SYMPOSIUM PROCEEDINGS VOLUME 157

Beam-Solid Interactions:
Physical Phenomena

Symposium held November 27-December 1, 1989, Boston, Massachusetts, U.S.A.